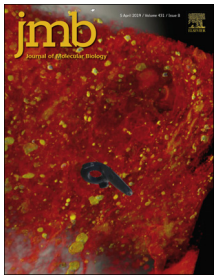

NapA (Rv0430), a Novel Nucleoid-Associated Protein that Regulates a Virulence Operon in *Mycobacterium tuberculosis* in a Supercoiling-Dependent Manner

Chandreyee Datta [1], Rajiv Kumar Jha [1], Sohini Ganguly [1] and Valakunja Nagaraja [1,2]

*1 - **Department of Microbiology and Cell Biology,** Indian Institute of Science, C.V. Raman Avenue, Bangalore 560012, India*
*2 - **Jawaharlal Nehru Centre for Advanced Scientific Research,** Bangalore 560064, India*

***Correspondence to Valakunja Nagaraja:** Department of Microbiology and Cell Biology, Indian Institute of Science, C.V. Raman Avenue, Bangalore 560012, India. vraj@iisc.ac.in*
https://doi.org/10.1016/j.jmb.2019.02.029
Edited by Anthony Maxwell

Abstract

Comparison of *Mycobacterium tuberculosis* with *Escherichia coli* reveals a reduction in the diversity of DNA-managing proteins, such as DNA topoisomerases, although genome sizes are similar for the two species. The same is true for nucleoid-associated proteins (NAPs), important factors in bacterial chromosome compaction, chromosome remodeling, and regulation of gene expression. In a search for still uncharacterized NAPs, we found that *M. tuberculosis* protein Rv0430 has NAP-like features: it binds to DNA in a length- and supercoil-dependent fashion, prefers A/T-rich DNA sequences, protects DNA from damaging agents, and modulates DNA supercoiling. At a ratio of 1 dimer/40 bps of DNA, Rv0430 bridges distant DNA segments; at 1 dimer/20 bps, it coats DNA, forming inflexible rods. Rv0430 also stimulates the DNA relaxation activity of topoisomerase I. Remarkably, Rv0430 stimulates its own promoter in a supercoil-dependent manner. It is the first gene of an operon harboring two regulators of *M. tuberculosis* virulence (*virR* and *sodC*), and controls the expression of these downstream virulence regulators and therefore itself is a virulence regulator. The sensitivity of *rv0430* expression to supercoiling is consistent with supercoiling being important for infection by *M. tuberculosis*. Thus, Rv0430 is a novel NAP, doubling up as a topology modulator of *M. tuberculosis*.

© 2019 Elsevier Ltd. All rights reserved.

Introduction

In bacteria, the task of packaging the chromosome is achieved by a combination of factors that include DNA topology, macromolecular crowding, and a set of small, basic, DNA-binding proteins called nucleoid-associated proteins (NAPs) [1–5]. Through a subtle interplay with conventional transcription factors, NAPs modulate gene expression [6]. Although all NAPs perform similar cellular functions of DNA organization and gene regulation, they come with unique properties. Some NAPs, such as IHF and Fis, are sequence-specific binders [7–9]; some, such as HU, do not discriminate between DNA sequences [10], while others, like H-NS, prefer A/T richness [11,12]. NAPs are versatile DNA-binding "architects" of chromosome structure [13] that in many cases alter the spatial trajectory of DNA [14]. They exhibit varied DNA-binding modes. For example IHF bends DNA, Lrp wraps DNA, and H-NS bridges and stiffens DNA in a concentration-dependent way [15–20]. Such "DNA sculpting" features impart NAPs with global gene expression regulatory abilities, which also extend to regulation of virulence factors in pathogenic organisms [13,21–24].

Interestingly, the number of NAPs varies among species. Particularly striking is the comparison of *Escherichia coli* with *Mycobacterium tuberculosis* (*Mtb*): *E. coli* and related bacteria contain at least 14 NAPs [25–27], while only half that number has been found in *Mtb* [28–34]. The most extensive work on NAPs has focused on the HU, H-NS, Fis, IHF, and Dps proteins of *E. coli* [6,35–39]. Other notable NAPs (Lrp, StpA, Hfq, and CbpA) of *E. coli* serve as transcription regulators for a large number of genes [40–42]. NAPs absent in *Mtb* are indeed among the best known of NAPs of *E. coli*, such as Fis, and Hfq [6], while some *Mtb* NAPs, like GroEL1, Lsr2, and EspR, are absent in gram-negative organisms [6]. *Mtb* NAPs, for example, H-NS (Rv3852 in *Mtb*) and

IHF (mIHF in *Mtb*), have different properties in the two organisms [32,34]. Notably, NAPs common to *E. coli* and *Mtb*, such as HU, are essential in the latter but not in the former [43,44], rendering them potential drug targets [43]. Thus, the study of *Mtb* NAPs is likely to expand our understanding of this important class of proteins, possibly opening up avenues to combat the pathogen.

The paucity of NAPs in *Mtb* and the large number of uncharacterized genes in this pathogen encouraged a search for novel NAPs that uncovered Rv0430, a small, basic, DNA-binding protein of unknown function. Purification and biochemical characterization of the protein revealed properties characteristic of NAPs. Two particularly interesting features emerged. First, Rv0430 regulates its own operon, which also contains two virulence genes (*virR*, *sodC*); thus, Rv0430 is a virulence regulator. Second, Rv0430-mediated regulation is supercoiling dependent; it activates expression from a supercoiled promoter while repressing it from a relaxed promoter. These observations raise the interesting possibility that changes in DNA supercoiling are important during infection by *Mtb*.

Results

Rv0430 is a dimeric DNA-binding protein

To identify novel *Mtb* NAP*s*, we examined the Mycobrowser database (https://mycobrowser.epfl.ch/) for *Mtb* proteins having a basic p*I*, small size (30–10 kDa), and an absence of annotated function. The gene product of *rv0430* satisfied the above criteria. Also, it was present in a multigene operon having downstream virulence regulators: *rv0430* is the first gene of an operon containing four other genes *virR*, *sodC*, *rv0433*, and *rv0434* (Fig. 1a). Transposon insertion analysis had suggested that *rv0430* is essential [45,46]. The gene is highly conserved among actinomycetes, but it is absent from gram-negative and other gram-positive bacteria (Fig. 1b).

Secondary and tertiary structure analysis indicated that Rv0430 might be a dimer containing a DNA-binding helix-turn-helix motif (Fig. S1a, b). Rv0430 was expressed and purified from *E. coli* and *Mycobacterium smegmatis* (Fig. S1c). The CD spectral analysis of Rv0430 indicated high alpha helical content that matched structural predictions (Fig. S1d). Glutaraldehyde crosslinking and gel filtration analysis established that Rv0430 exists as a dimer in solution (Fig. 1d, e).

Electrophoretic mobility shift assay (EMSA) experiments revealed that the protein binds to linear, relaxed, and supercoiled forms of pUC18 DNA, with greater binding to the supercoiled form (Fig. 2a). The *Mycobacterium gilvum* homologue of Rv0430, which shares 90% identity with *Mtb* Rv0430, is annotated as belonging to the Fis family. Hence, DNA binding was assessed using oligonucleotides containing a consensus sequence for *E. coli* Fis. The protein formed complexes with the double-stranded FBS30-mer and FBS60-mer oligonucleotides (Supplementary Table S1), both of which contain a binding site for Fis (Fig. 2bi, ii) [47]. To examine further binding properties of Rv0430, two other double-stranded oligonucleotides of different lengths, GRA31 and GRA51 (31 and 51 nucleotides long, respectively), which represented regions of the *Mtb* genome but without the Fis binding sequence (Supplementary Table S1), were used. While Rv0430 formed complexes with these sequences (Fig. 2cii, iii), the protein failed to form complexes with a double-stranded GRA19 (19-mer oligonucleotide) (Fig. 2ci). Other unrelated 13-mer and 19-mer double-stranded oligonucleotides also did not bind to Rv0430. Single-stranded DNA was found to be not a substrate for Rv0430 binding (data not shown). From these studies, it is apparent that Rv0430 is a DNA-binding protein, and its interaction with DNA appears to depend on both the topology and length of the DNA.

Rv0430 prefers A/T-rich DNA sequences

Although NAPs are usually sequence independent DNA-binding proteins, some show a preference for particular sequences. To investigate the sequence dependence of Rv0430, six rounds of selective evolution of ligand by exponential enrichment (SELEX) were carried out with both Rv0430 and its orthologue from *M. smegmatis*, MS_0833. MS_0833 shows 85% sequence identity with Rv0430 (Fig. 3a). No enrichment was observed beyond the fifth round of SELEX. EMSA with a radiolabeled enriched oligo pool of the fifth and sixth SELEX rounds with Rv0430 (Fig. 3b) and MS_0833 (Fig. 3c) showed formation of DNA–protein complexes. To identify the sequence of the enriched oligonucleotides, sequencing of the DNA obtained in the sixth round was performed. Although the DNA molecules sequenced showed heterogeneity, they were A/T rich. All the sequences obtained after six rounds of SELEX had at least one contiguous stretch of four A/Ts; however, most of the sequences had longer A/T stretches, sometimes interrupted with one G or C (Table 1).

To corroborate the SELEX results, filter-binding assays were carried out with oligonucleotides having varying A/T content. The filter-binding studies showed higher affinity of Rv0430 and MS_0833 for the SeL_1 and SeL_2 oligonucleotides (73% AT) relative to the SeL_3 oligonucleotide (30% AT) (Fig. 3d) (Supplementary Table S1).

Rv0430 protects DNA from damaging agents

During infection, *Mtb* experiences DNA-damaging stress when inside macrophages. DNA-binding proteins, such as Lsr2, have been implicated in physically

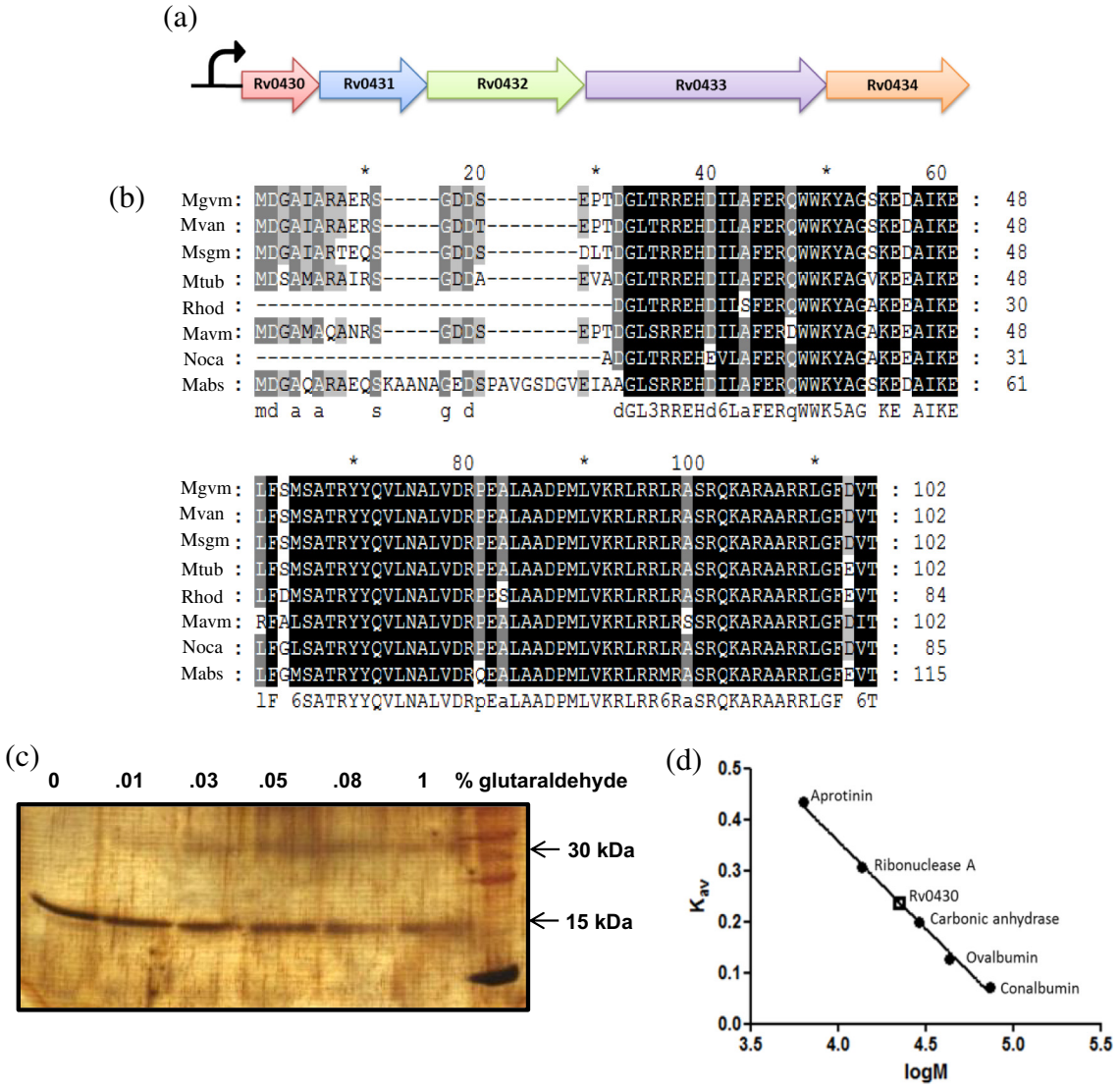

Fig. 1. The dimeric Rv0430 is encoded from the first gene in a five gene operon. (a) Genomic organization *rv0430*. *rv0430* is a part of a five gene operon (the *rv0430* operon). It is the first gene of the operon followed by *virR*, *sodC*, *rv0433*, and *rv0434*. (b) Multiple-sequence alignment of Rv0430 showing its conservation within the actinobacterial species. (c) Rv0430 was crosslinked with different concentrations of glutaraldehyde (0 to 1%) and electrophoresed on a 15% SDS-PAGE. The crosslinked band indicates the dimeric nature of Rv0430. (d) Analytical gel filtration. Rv0430 was eluted through a superdex G75 column. The K_{av} ($V_e - V_0/V_c - V_0$, where V_e is elution volume; V_0, column volume; V_c, void volume) value of Rv0430 with that of the known molecular weight standards was compared. The open square represents the calculated K_{av} value for Rv0430. The interpolated molecular weight corresponds to 22.5 kDa, while the theoretical monomeric molecular weight of Rv0430 is 11.7 kDa, suggesting that Rv0430 exist as a dimer.

protecting *Mtb* DNA from peroxide-mediated damage [48]. The stationary-phase-specific DNA-binding protein Dps also plays a significant role in protecting DNA from oxidative radicals and other damaging agents [49]. When the ability of Rv0430 to protect DNA from the action of DNA damaging agents was examined, it protected both supercoiled and linear pUC18 DNA from the enzymatic activity of DNaseI (Fig. 4ai, ii). It also protected pUC18 DNA from the action of radicals generated by the Fenton reaction. Supercoiled pUC18 undergoes complete degradation in the presence of $FeSO_4$ and H_2O_2 (see Materials and Methods). When incubated with Rv0430, complete degradation was prevented, although nicks were observed (Fig. 4b). Thus, binding of Rv0430 to DNA physically protects it from the action of two DNA-damaging agents.

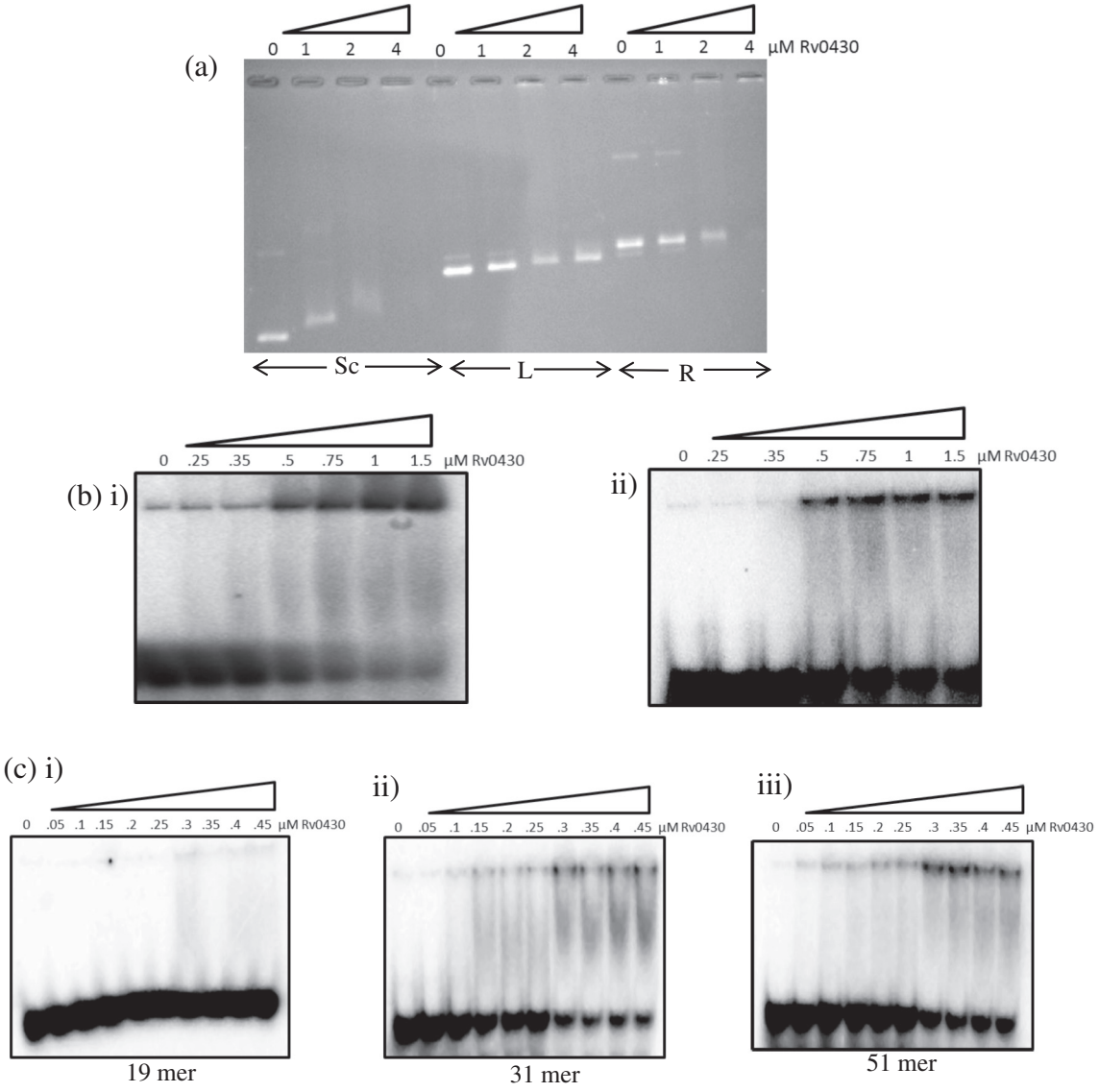

Fig. 2. Rv0430 binds to DNA in a length- and topology-dependent manner. (a) Rv0430 at different concentrations (0 to 4 μM) was incubated with supercoiled (Sc), relaxed (R), and linear (L) pUC18 DNA. DNA–protein complexes were resolved on 1% agarose gel stained with EtBr. (b) Rv0430 at different (0 to 1.5 μM) concentrations was incubated with 5′ ^{32}P labeled (i) 31-bp double-stranded DNA and (ii) 60-bp double-stranded DNA containing a Fis binding sequence (FBS30, FBS60). DNA–protein complexes were resolved on 6% non-denaturing polyacrylimide gel. (c) To analyze the dependence of Rv0430 binding on the length of DNA, it was incubated with 5′ ^{32}P-labeled (i) 19-bp, (ii), 31-bp, and (iii) 51-bp double-stranded DNA representing regions from *Mtb* genome. DNA–protein complexes were resolved on 6% non-denaturing polyacrylimide gel. Experiments were carried out thrice with similar results. Representative images are shown.

Rv0430 is a DNA-topology modulator and a DNA-architectural component of chromosomes

NAPs are known to bind to DNA in a variety of ways that change the DNA spatial trajectory. We investigated the architectural effects of Rv0430 on DNA using atomic force microscopy (AFM). When relaxed and linear DNA were incubated with Rv0430 at a concentration of one protein dimer per 40 bp, intramolecular bridging was observed (Fig. 5b, c). The height of the protein-bound region of DNA was in the range of 1 to 1.2 nm, while that of DNA alone was 0.3 nm (Fig. 5a). The Rv0430 homologue from *M. smegmatis*, MS_0833, showed similar bridging properties (Fig. S2).

AFM images of DNA–protein complexes, at the higher relative concentration of one Rv0430 dimer per 20 bp, showed complete coating of the DNA by Rv0430 (Fig. S3a). To corroborate DNA coating, an end-joining

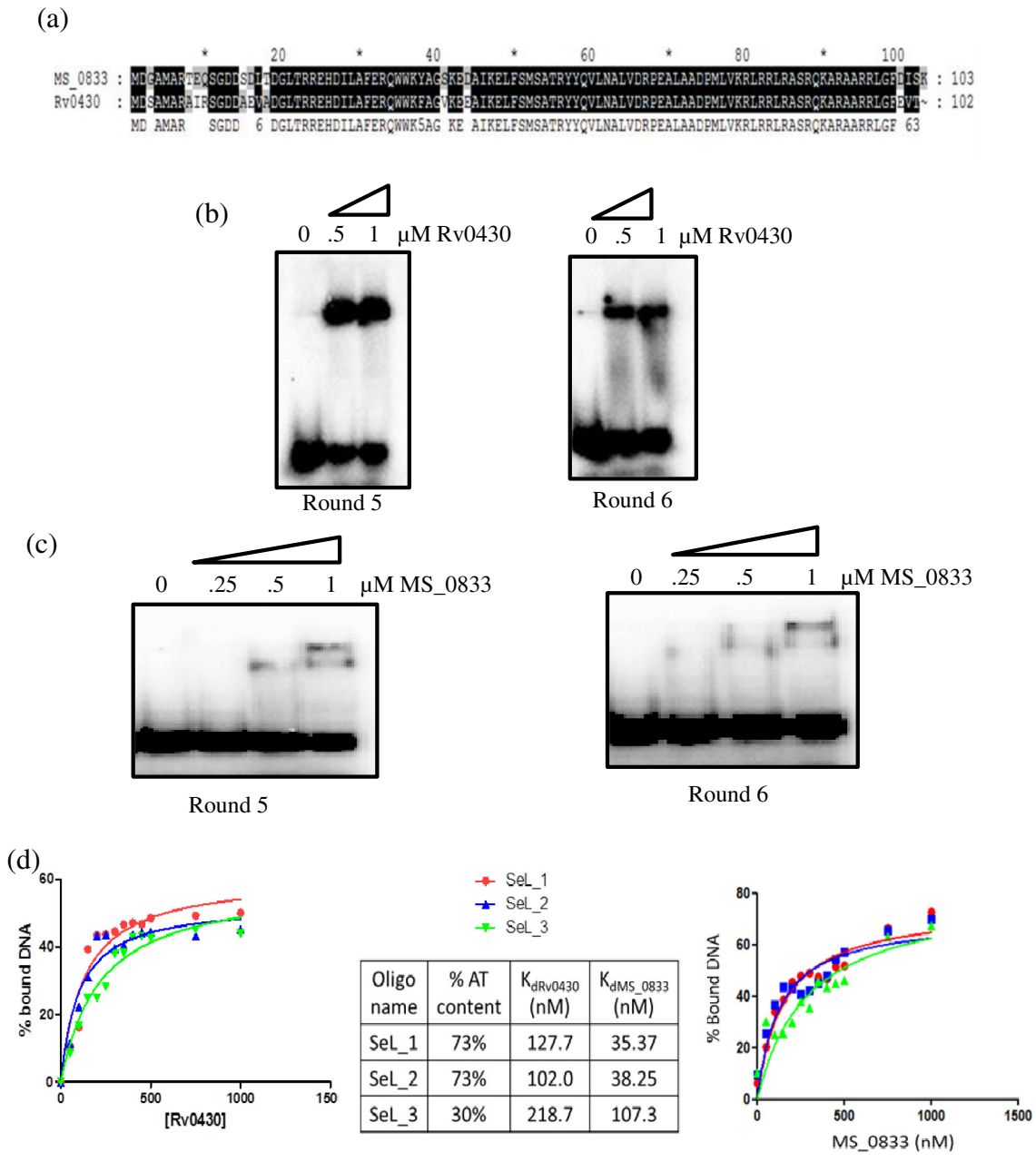

Oligo name	% AT content	$K_{dRv0430}$ (nM)	K_{dMS_0833} (nM)
SeL_1	73%	127.7	35.37
SeL_2	73%	102.0	38.25
SeL_3	30%	218.7	107.3

Fig. 3. SELEX analysis showing the preference of Rv0430 for A/T-rich DNA. (a) Pairwise sequence alignment of Rv0430 and MS_0833 showing 85% identity. (b) EMSA was carried out by incubating the radio-labeled pool of SELEX-enriched oligonucleotides of the fifth and sixth rounds with Rv0430. The resulting complexes were resolved on 6% non-denaturing polyacrylamide gel. (c) EMSA was carried out by incubating the radio-labeled pool of SELEX-enriched oligonucleotides of the fifth and sixth rounds with MS_0833. The resulting complexes were resolved on 6% non-denaturing polyacrylamide gel. List of oligonucleotide sequences after six rounds of SELEX of Rv0430 and MS_0833 (Table 1) shows the preference of the proteins for A/T-rich sequences. (d) Affinity of Rv0430 and MS_0833 of oligonucleotides of varying A/T richness (SeL_1, SeL_2, SeL_3) was analyzed by filter-binding assay. The mean of readings from three independent experiments was plotted. (K_D values are indicated in tabular form.)

assay was carried out wherein the ligation of cohesive ends of a linearized pUC18 DNA was monitored in the presence and absence of Rv0430. At one Rv0430 dimer per 20 bp, the amount of the monomeric circular species of DNA was reduced, while the amount of dimeric and trimeric intermolecularly ligated species increased (Fig. S3b). It is evident that at higher relative concentrations (1 Rv0430 dimer: 20 bp), the protein binds throughout the DNA, thereby coating and stiffening linear DNA. This effect prevents DNA

Table 1. Table listing the sequences obtained after the sixth round of SELEX with Rv0430 and MS_0833

Rv0430	MS_0833
GAAGTGTAATTAAGGGTGT	GTGTTCCTTTCGTTAAGT
CAGATAAACCATACATGT	CCCCTGTTTTCTCCGTGG
TATCTAATCACCTCCCTG	ACTGGATTAAAAGACAAC
GTACAATAGGGGGTGGAC	CCAATAACTTTGGTCTCT
TTCTAAAAACCAGGGTGT	TCTTAGGAGATATAGAAT
GCCATGAGTGTTTTGCAG	GATACTTTACTTACAATA
CGCGGTTCTGATAACTTT	CAACTCTTTCTTTTATGA
ATATTTGTAAATATTTTC	TGTCTATCTAATATTTAC
GAAAAAAGGTAGAGGACG	TCCGTTGAATTATGGTTG
AACCCAGCAACAATTACC	TAACTAAAGTACAAACCG
CGAGGTTAGTCTTTAGTC	CACTTCATGATATATTAT
ATTTTTTTTAGCTGCTTT	GCAAACTGCTTAAAGTAG
GCCCATAAATATTCGTTA	AAAATATGGTTTTTCCCC
ATATAAACTTTTTCAGT	ACAAAACTTTGTAGAGGG
CACAAAACCGTCTTTTCG	GTACGGCAATTTATTGTA
GAAATATGTGTCTGTGTT	GGATATATCTACAGTGTC
GGCAAGTTTGACAAGTAG	AAAAACCCGCATCCTTAG
GGATATGTTCGTTCTGCA	CATTACGAAGAAACCAT
CCCCCAATTTTCTTTTTC	GTATTCAATGCTTATTTA
AAAAGCACATAAATCCCC	CCTTAATCATTTTTTTAC
CTCAACTTCTTTTCACCG	ACAATAAAAATCCATGTG
CTTTCCCCTATCAATGAT	AACAGTAAAATTCAAGTC
GGATGACGAGTTTTGGGC	AACAGTAAAATTCAAGTC
CATTATTTTACCCATGGT	TTACGAAAATAAAGCGGG
ATTTACTTTATGCTTTAT	AAACGATTACTTCCGTAC
TGTAATATATAATGCCTA	ACAATATAAAAGAAGTGG
	TACTATCAATAAATGTGC
	CAAACTTTTTTATTGATA
	CCCAGGTAGATTAGTTTC
	TATTATAATAACAAGTGT

circularization and facilitates intermolecular ligation relative to intramolecular ligation. Together, these results indicate that at lower protein:DNA ratios, Rv0430 can bridge DNA, bringing together two distant DNA segments, while at high ratios, it coats and stiffens DNA into rod-like structures.

To examine the effects of Rv0430 on DNA supercoiling, DNA relaxation assays were carried out with type IA topoisomerases. Rv0430, at lower concentrations (1 dimer per 1280 bp to 1 dimer per 64 bp), stimulated the relaxing activity of both mycobacterial and *E. coli* topoisomerase I (Fig. 6a, b). This stimulation is thus not species-specific, unlike stimulation of *Mtb* topoisomerase I by MtHU [50].

Rv0430 regulates transcription from its own promoter in a supercoil-dependent manner

Since Rv0430 is the first gene of its operon and possesses DNA-binding ability, we suspected that it might have a regulatory role. The promoter of this operon has an A/T tract, a potential Rv0430 binding site. The protein bound to a radiolabeled promoter fragment of the *rv0430* operon, consistent with an ability to directly interact with its own promoter (Fig. 7ai, b). Whole-cell chromatin immunoprecipitation (ChIP), using antisera directed against Rv0430, also showed enrichment at the *rv0430* operon promoter (Fig. S4).

To examine the regulatory ability of Rv0430, *in vitro* transcription reactions were carried out from the promoter (Fig. 7aii) in the presence or absence of Rv0430. When the promoter was present on a relaxed or linear DNA, transcription was progressively inhibited by increasing concentrations of Rv0430 (Fig. 7ci, ii). However, with negatively supercoiled DNA, Rv0430 stimulated transcription (Fig. 7ciii). Thus, Rv0430 may have an auto-regulatory role that is influenced by promoter topology.

To determine whether this topology-dependent regulation occurs *in vivo*, *Mtb*H37Ra cells were treated with the DNA gyrase inhibitor novobiocin (which relaxes chromosomal DNA[51]). DNA relaxation in turn leads to transcriptional upregulation of gyrase expression to restore the topological equilibrium of the cell, a phenomenon known as relaxation stimulated transcription (RST) [52]. We exploited this effect as a tool to investigate the supercoil-dependent auto-regulation at the *rv0430* promoter. Previous studies showed that the RST response in *Mtb* is seen after 12–24 h of novobiocin treatment [53]. We also observed gyrase upregulation at 24 h, but not after 4 h of novobiocin treatment (Fig. S5). Thus, after 4 h of novobiocin treatment, the *Mtb* genome should be relaxed compared to the untreated condition. Under such conditions, mRNA levels of *rv0430* and *rv0431* were downregulated. After 24 h, mRNA levels of gyrase increased, indicating establishment of RST and restoration of DNA supercoiling. At this time point, mRNA levels of *rv0430* and *rv0431* were higher than at 4 h (Fig. 7di, ii). Increased mRNA levels of *rv0430* and *rv0431* at 24 h, relative to that at 4 h of novobiocin treatment, indicated that the operon is downregulated when the chromosome is relaxed and upregulated when supercoiled. This is in agreement with the results of the *in vitro* transcription reaction.

Discussion

NAPs, thought to be the prokaryotic histone counterparts, are bacterial chromatin-architectural proteins. Through their various DNA-binding modes, changes in concentrations in response to external stimuli, and their ability to modulate DNA supercoiling, NAPs help maintain nucleoid shape and dynamics [5,6,54,55]. The experiments described above identify a novel NAP, Rv0430 (*N*ucleoid-*a*ssociated *p*rotein with *a*uto-regulatory activity, or NapA), which participates in regulation of virulence genes in *Mtb*. NapA is a DNA-architectural protein with concentration-dependent, distinct DNA-binding modes and a DNA-topology modulator. It shows supercoiling-dependent regulatory activity at its promoter that drives expression of important virulence regulators (*virR* and *sodC*). The present work not only adds a new NAP to those characterized for *Mtb* but also identifies a novel virulence factor of *Mtb*.

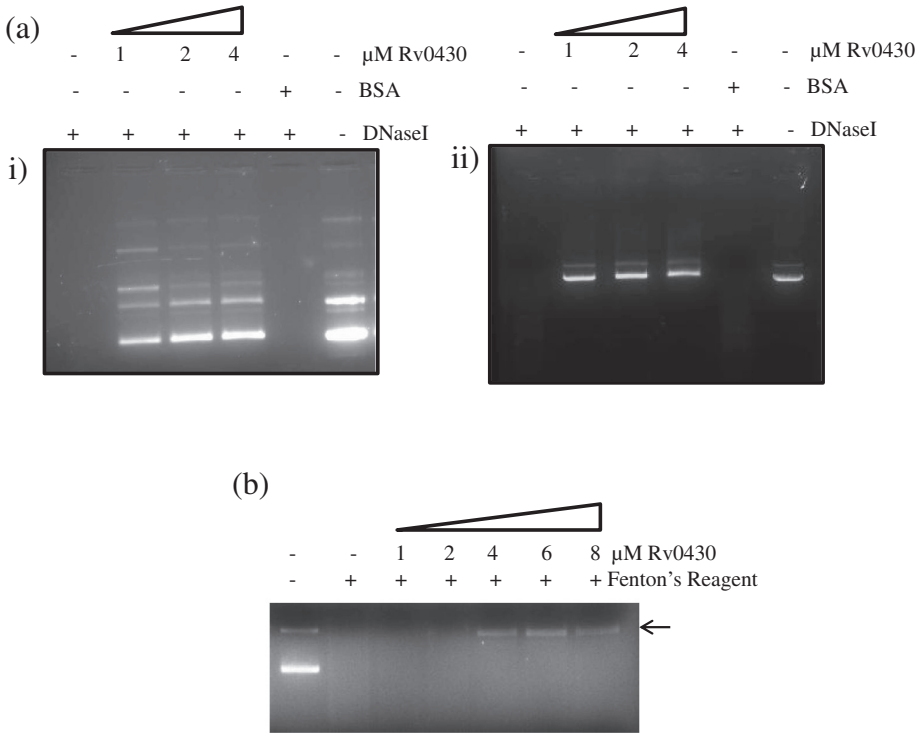

Fig. 4. Rv0430 protects DNA from the action of DNA-damaging agents. (a) Rv0430 was incubated with (i) supercoiled and (ii) linear pUC18 DNA and subjected to DNase I treatment. Reactions were electrophoresed on a 1% agarose gel stained with EtBr. Prevention of degradation is observed on incubation with Rv0430. (b) Rv0430 was incubated with supercoiled pUC18 DNA and subjected to peroxide radicals generated by Fenton's reaction. Reactions were electrophoresed on a 1% agarose gel stained with EtBr. Prevention of degradation is observed on incubation with Rv0430. Complete degradation is prevented on incubation with Rv0430 as observed by the nicked pUC18 band (marked by arrow). Experiemnts were carried out three times with similar results. Representative images are shown.

The role of NAPs as DNA organizers arises from their ability to bind DNA in a varied manner [14]. Although usually promiscuous DNA binders, some NAPs show a preference for particular sequences. For example, H-NS binds preferentially to A/T-rich DNA, thereby playing a repressive role at the A/T-rich xenogeneic regions in *E. coli* and *Salmonella* [11,12,37]. Fis binds in a sequence-specific manner to a 15-bp A/T-rich sequence flanked by G/C and C/G base pairs [7], regulating a large number of *E. coli* promoters [56]. CbpA from *E. coli* binds to A/T-rich curved DNA sequences, allowing it to bind to the intrinsincally curved *ter* macrodomain [57]. Although the mycobacterial genome is G/C rich, the mycobacterial NAP Lsr2 binds to A/T-rich regions, playing a role similar to H-NS in gram-negative bacteria [58]. As revealed by our SELEX analysis, NapA too has a predilection for A/T-rich sequences. In the *Mtb* genome, there are distinct A/T-rich regions, which include some genomic islands [59], promoters, and regulatory regions. We therefore speculate that NapA may exhibit regulatory roles at such genomic locations. In fact, we demonstrate NapA binds to its promoter, which is A/T-rich, regulating its own expression.

Upon binding, NAPs induce architectural changes on the DNA (bending, bridging, wrapping, and coating) [14]. Some NAPs can switch their binding mode depending on the relative concentration or other external factors [20,60,61], which can lead to vastly different regulatory consequences. For instance, H-NS, at low concentrations, forms DNA bridges, trapping RNA polymerase and aiding in transcription termination, but at higher concentration, it coats the DNA, forming filaments and thus cannot trap the polymerase [20]. Such sculpting of the DNA by NAPs is important not only for compaction and local structural changes but also for maintenance of topologically independent DNA loops. Our results show that NapA also has DNA sculpting properties. Moreover, its architecturing ability is dependent on concentration. It binds and brings distant DNA regions closer, forming bridges and loops at low concentrations (1 dimer per 40 bp). At higher concentration (1 dimer per 20 bp), it coats the DNA forming filaments. Indeed we see prevention of circularization and stimulation of intermolecular ligation of DNA in the presence of higher concentration of NapA, possibly a consequence of DNA stiffening. This observation thus opens up an interesting question on

the binding mode of NapA in the cell. Depending on local concentrations or growth phase-dependent expression, NapA could exhibit either bridging or stiffening leading to different structural consequences. From the data presented, it is apparent that NapA can alter DNA structure upon binding by its different binding modes, thus suggesting an active role in chromosome modeling.

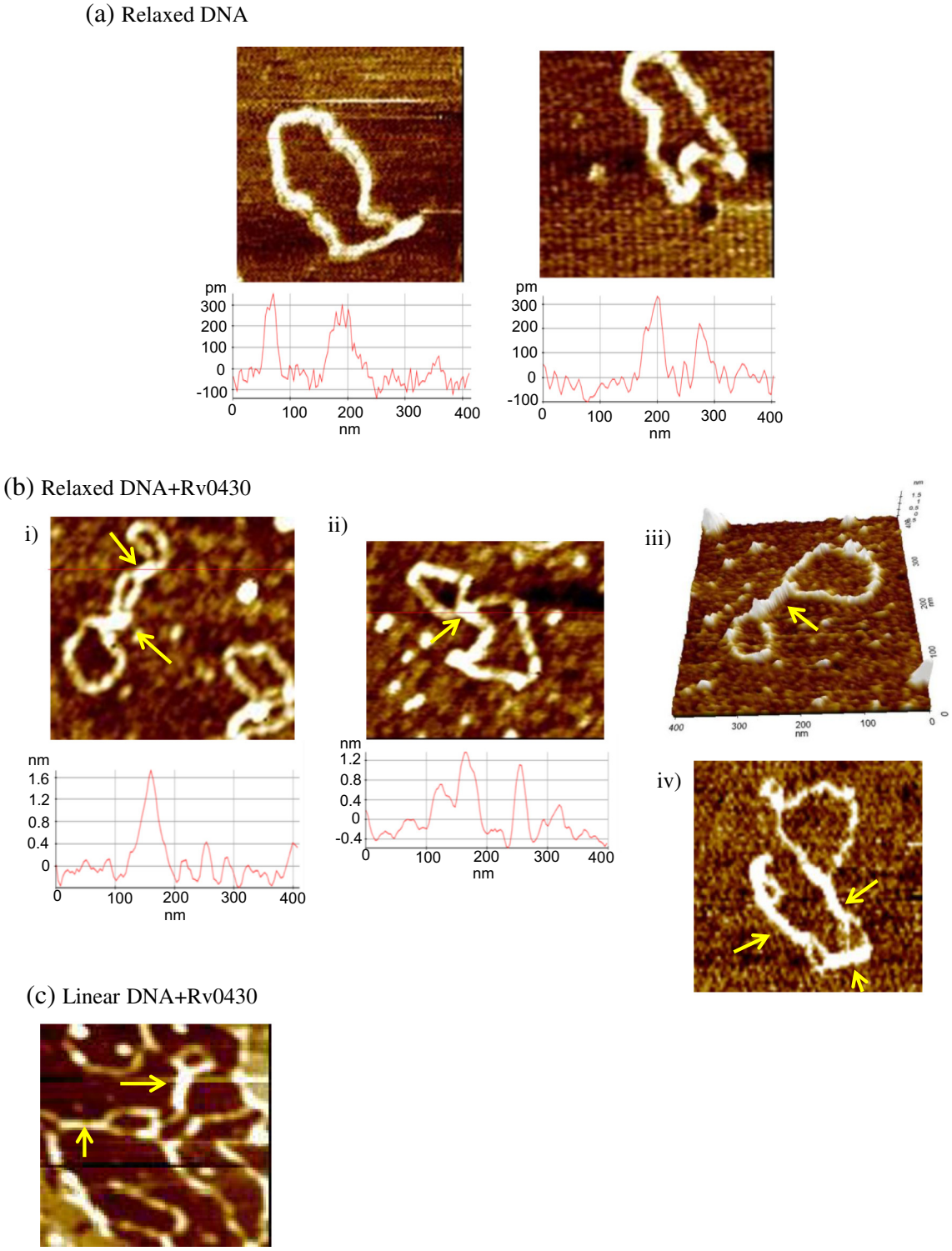

Fig. 5 (*legend on next page*)

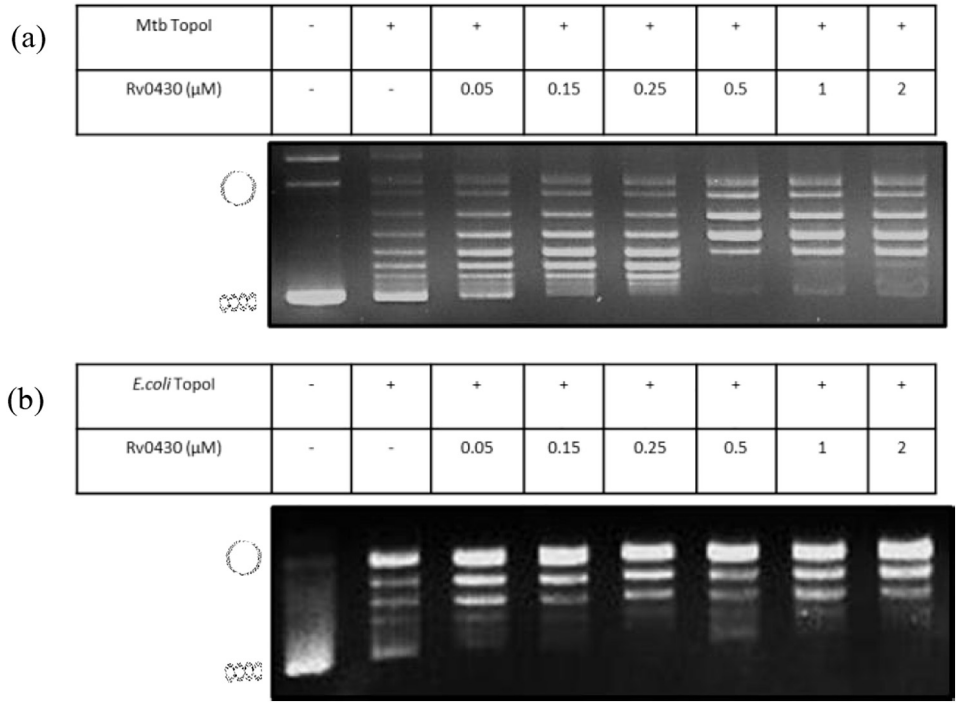

Fig. 6. Rv0403 can modulate DNA topology. DNA relaxation assays were carried out in the presence of Rv0430. Supercoiled pUC18 DNA and the indicated amounts of Rv0430 were incubated followed by relaxation with topoisomerase I. The topoisomers were resolved on 1.2% agarose gel and visualized by EtBr staining. Increase in the amount of relaxed products was observed in the Relaxation assays with (a) *M. tuberculosis* topoisomerase I and (b) with *E. coli* topoisomerase I.

NapA also modulates DNA supercoiling, as seen by its ability to stimulate TopoI activity. The *E. coli* NAP HU, is also a topology modulator, constraining negative supercoils into DNA [62]; mutation in one of its amino acids ($HU\alpha^{+}\beta E38A$) can compromise this topology modulation activity [62]. Another HU mutant (HUαE38K,V42L) restrains positive supercoils [63] and causes increased global supercoiling in *E. coli* resulting in massive transcriptional rewiring [64]. *Mtb* HU, on the other hand, functions as a topology modulator by interacting with and thereby stimulating the activity of *Mtb* TopoI [50]. NapA probably modifies DNA topology upon binding, rendering DNA a better substrate for Topo I to act upon. This influence on DNA topology could have regulatory consequences for DNA transaction processes; introduction of negative supercoils would open up promoter regions to facilitate RNA polymerase (RNAP) binding [65,66].

Chromosome supercoiling is a critical determinant in transcriptional regulation [67]. Each step of the transcriptional process is influenced by the supercoiling status of DNA. The role of DNA topology in the regulation of virulence genes in bacteria has been discussed for many years [68]. NAPs and transcription factors contribute to supercoiling changes in response to external stimuli [69], thus regulating expression of genes associated with pathogenesis. For example, a complex mechanism involving H-NS- and Fis-mediated supercoiling modulation of the *pelE* promoter operates in the plant pathogen *Dickeya dadantii* [70,71]. In *Salmonella*, Fis facilitates stabilization of different superhelical densities of the chromosome, thus aiding in timely expression of the pathogenicity islands [23,71]. Although *Mtb* appears to have fewer number of NAPs, some of them are shown to be involved in regulation of virulence genes. Lsr2 binds to

Fig. 5. Rv0430 is a DNA-bridging protein. pUC18 DNA was incubated with Rv0430 at concentration of 1 protein dimer per 40 bp. The DNA–protein complexes were visualized by AFM. (a) AFM images of relaxed circular pUC18 DNA. The scan at the bottom represents the trace of the AFM cantilever along the red line in the AFM image. The peak represents the height of naked DNA (~0.3 nm). (b) AFM images of relaxed circular pUC18 DNA–Rv0430 complexes showing bridged regions indicated by arrows. (i, ii) AFM images of DNA–Rv0430 complexes along with horizontal height scans (along the horizontal red line in the image) at the bottom showing increased heights of protein bound bridged DNA regions (~1.5 nm). (iii) AFM image of DNA–Rv0430 complex represented in 3D. (iv) AFM image of DNA–Rv0430 complex. (c) Linear pUC18 DNA was incubated with Rv0430 at a concentration of 1 protein dimer per 40 bp. AFM image showing bridging of linear DNA by Rv0430. (All images are 400 × 400 nm in dimension.)

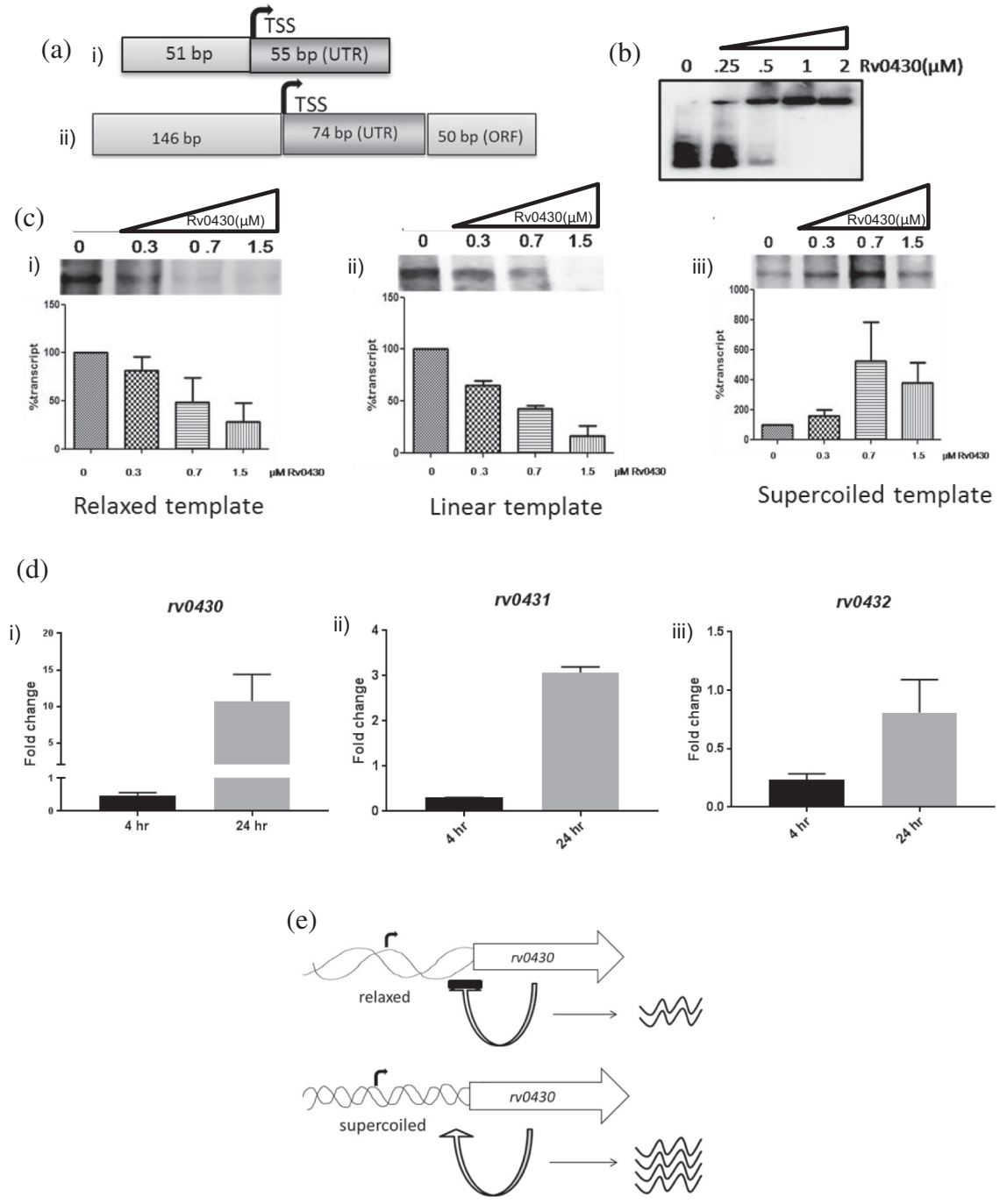

Fig. 7. DNA topology-dependent auto-regulation of Rv0430. (a) *rv0430* promoter fragment used for (i) EMSA and (ii) *in vitro* transcription assays. (b) Rv0430 binds to its own promoter. *rv0430* upstream sequence (ai) was incubated with Rv0430 and the resulting complexes were analyzed on a 6% non-denaturing polyacrylimide gel. (c) *In vitro* transcription reactions was carried out with *rv0430* promoter (aii) cloned in pARN vector. Reactions were carried out with (i) relaxed, (ii) linear, and (iii) supercoiled forms. The transcripts were electrophoresed on a 6% urea-PAGE (the quantification from three independent *in vitro* transcription experiments is given along with the representative gels). (d) Chromosomal DNA supercoiling in *Mtb*H37Ra was perturbed with the DNA gyrase inhibitor, Novobiocin. Increased expression of DNA gyrase after 24 h and not after 4 h of novobiocin treatment (Fig S5) suggests increased genome supercoiling at 24 h when compared to 4 h. Increased expression of the genes of the *rv0430* operon, *rv0430* and *rv0431*, at 24 h as compared to 4 h shows transcription activation by Rv0430 from supercoiled DNA. (e) Model representing topology dependent auto-regulation of the *rv0430* operon by Rv0430

and regulates myriad genes including several involved in pathogenesis [58,72]. EspR regulates the *espACD* operon, which is required for normal functioning of the ESX-1 secretion system [73], while NapM regulates genes responsible for drug sensitivity and resistance [33].

NapA, the new addition to the *Mtb* NAP list, is the first gene product of a multi-gene operon. The second (*virR*) and third (*sodC*) genes of this operon are known *Mtb* virulence regulators. VirR regulates formation of membranous vesicles, which carry lipoprotein and immuno-modulatory cargo to the host [74]; its mutation causes attenuated infection in mice [75]. One of the proteins transported by these vesicles is the third-gene product of the operon, SodC. SodC, a membrane-tethered superoxide dismutase, counters the oxidative stress that the bacteria face inside the macrophage [76]. Its expression increases several fold in human macrophages upon infection, and a *sodC* null mutant is compromised in survival when exposed to externally generated oxidative stress [77,78]. Thus, the *rv0430* operon seems to be crucial for the virulence of *Mtb*.

We show the supercoiling-dependent autoregulation of NapA, wherein transcription repression results from a relaxed promoter and supercoiled promoter cause stimulation in transcription in the presence of NapA. It appears that being a topology modulator, NapA modulates the supercoiled promoter in a manner that facilitates transcription. It seems conceivable that environmental stimuli-induced changes in the supercoiling level of the *rv0430* promoter can cause its regulation by NapA, thereby changing the levels of the downstream virulence genes. However, other unidentified components acting in concert with NapA may fine tune the expression of the operon.

To conclude, NAP-mediated chromatin remodeling governs survival and pathogenesis in several bacteria. The mycobacterial nucleoid is organized and managed by the concerted action of topoisomerases and various NAPs. Although annotated to be a "Fis" family of regulator, properties of NapA indicate its distinctiveness. In high-density transposon mutagenesis studies, *napA* (*rv0430*) mutant was not found, suggesting its essentiality in *Mtb* [45,46]. Present studies suggest that NapA is indeed a crucial mycobacterial NAP capable of modulating DNA structure and supercoiling, also doubling up as a regulator of its own operon, which is important for virulence.

Materials and Methods

Strains and growth media

M. smegmatis cultures were grown in 7H9 media (Difco, USA) containing 0.4% glucose and on 7H11 agar (Difco, USA) containing 0.4% glucose and 0.05% Tween-80. *Mtb*H37Ra cultures were grown in 7H9 media containing 0.2% glycerol, 0.05% Tween-80, and 1× albumin dextrose catalase, and on 7H11 agar with 0.2% glycerol and 1× oleic acid albumin dextrose catalase.

Cloning of *rv0430* and *ms_0833* and expression/purification of their protein products

The coding region of *Mtb rv0430* was amplified by PCR using primers Rv0430FP1 and Rv0430RP2 (Supplementary Table S1). It was then inserted into pET20b(+) (Novagen) between the NdeI and XhoI sites to create pET20b-Rv0430 such that a hexa-histidine tag was placed at the carboxy terminus of Rv0430. The protein was expressed in *E. coli* BL21 (DE3) by adding 0.3 mM IPTG to cultures for inducing expression. The cells were suspended in lysis buffer [10 mM Tris–HCl (pH 7.4), 5% glycerol, 1M NaCl, 0.2 mM phenylmethylsulfonyl fluoride (PMSF)] and lysed with a sonicator using a macro probe set at 50% of the duty cycle for 7 min at 4 °C.

For cloning into the mycobacterial expression vector pMyNT, the coding regions of *ms_0833* and *rv0430* were amplified using the primers MS_0833FP and MS_0833RP for *ms 0833* and Rv0430FP2 and Rv0430RP2 for *rv0430* (Supplementary Table S1) and inserted into the pMyNT vector (a gift from Annabel Parret & Matthias Wilmanns (Addgene plasmid no. 42191)) between the NcoI and HindIII sites to create pMyNT-MS_0833 and pMyNT-0430, respectively, each with a hexa-histidine tag at the amino terminus of the expressed protein.

Proteins were expressed in *M. smegmatis* by adding 2% acetamide to exponentially growing cultures for 6 h at 37 °C. Cell were lysed using French pressure cell in lysis buffer, the cell lysates were clarified by centrifugation at 20,000*g* for 30 min at 4 °C, and the supernatant fluid was incubated with Ni-NTA beads (G biosciences, USA) for 2 h at 4 °C. Protein-bound beads were washed with wash buffer I [10 mM Tris–HCl (pH 7.4), 5% glycerol, 500 mM NaCl, 0.2 mM PMSF] and wash buffer II [10 mM Tris–HCl (pH 7.4), 5% glycerol, 100 mM NaCl, 0.2 mM PMSF, 50 mM imidazole]. Proteins were then eluted with elution buffer [10 mM Tris–HCl (pH 7.4), 5% glycerol, 100 mM NaCl, 0.2 mM PMSF, 500 mM imdazole]. Protein-containing fractions were pooled and subjected to 50% ammonium sulphate precipitation. The protein was collected by centrifugation, dissolved in resolubilization buffer [10 mM Tris–HCl (pH 7.4), 100 mM NaCl, 5% glycerol, 0.2 mM PMSF], and total protein was determined by the method of Bradford.

Analytical gel filtration and gluteraldehyde crosslinking

Purified Rv0430 was loaded onto a prepacked Superdex75 column (GE Healthcare, USA) in buffer

containing 20 mM Tris–HCl (pH 7.4), 100 mM NaCl, 5% glycerol, and 0.2 mM PMSF at a flow rate of 0.25 ml min^{-1}. The column was calibrated using conalbumin (75 kDa), ovalbumin (44 kDa), carbonic anhydrase (29 kDa), RNaseA (13.7 kDa), and aprotinin (6.5 kDa) as standards (GE Healthcare, USA). The oligomerization status of Rv0430 was determined from a calibration plot using known molecular weights of the proteins listed above.

For crosslinking, Rv0430 was treated with various concentrations of gluteraldehyde in 20 mM Hepes (pH 7.4) and 50 mM NaCl buffer for 15 min at 25 °C. Reactions were terminated with stop dye (62.5 mM Tris–HCl, 1.5% SDS, 8.3% glycerol, 0.005% bromophenol blue) and analyzed by 15% SDS PAGE, with detection by silver staining.

Structural predictions and circular dichroism

CD spectra of Rv0430 (2 μM) were obtained using a Jasco J815 CD spectrophotometer in a wavelength range of 200 to 250 nm (path length and scan rate were 0.1 cm and 50 nm min^{-1}, respectively). A secondary structure prediction for Rv0430 was carried out using the PSIPRED workbench at http://bioinf.cs.ucl.ac.uk/psipred/ using FUGUE, which is a program for recognizing distant homologues by sequence-structure comparison. The Rv0430 amino acid sequence was submitted at http://mizuguchilab.org/fugue/prfsearch.html. The probable tertiary structure was modeled based on the structure of *Bacillus subtilis* protein GerE, the closest structural homologue in the FUGUE database.

EMSA and DNA protection assays

Single-stranded oligonucleotides GRA19, GRA31, GRA51, FBS30, and FBS60 (Supplementary Table S1) were labeled at the 5′ end using ATP-[γ-^{32}P] and T4 polynucleotide kinase (New England Biolabs, USA). The labeled oligonucleotides were converted to double-stranded oligonucleotides by annealing with the complementary oligonucleotides GRA19c, GRA31c, GRA51c, FBS30c, and FBS60c (Supplementary Table S1) in 1× annealing buffer [10 mM Tris–Cl (pH 7.5), 50 mM NaCl]. The resulting oligonucleotides were incubated with Rv0430 or MS_0833 in the presence of 1× EMSA buffer [10 mM Tris–Cl (pH 7.5), 100 mM NaCl, 5% glycerol] at 25 °C for 30 min. Electrophoresis of the samples was performed using 6% non-denaturing polyacrylimide gels in 0.5× TBE, and detection of DNA protein complexes was performed by phosphorimager (GE Healthcare, USA). To detect binding of Rv0430 to its promoter region, a 107-bp sequence upstream from the Rv0430 coding region was amplified by PCR using 5′ ATP-[γ-^{32}P]-labeled Rv0430_107FP and non-radioactive Rv0430_107RP (Supplementary Table S1). The resulting radiolabeled PCR amplicon was used for EMSA with Rv0430 as described above. Supercoiled, relaxed, and linearized pUC18 DNA samples were incubated with Rv0430 or MS_0833 in 1× EMSA buffer for 30 min at 25 °C. The DNA–protein complexes were analyzed after electrophoresis in a 1.2% agarose gel followed by staining with ethidium bromide (EtBr) and visualization with UV light.

To examine protection afforded by Rv0430 against DNaseI, pUC18 was incubated for 20 min at 25 °C with increasing concentrations of Rv0430 in 1× EMSA buffer (1 Rv0430 dimer for 40 bp to 1 Rv0430 dimer per 10 bp). One unit of DNaseI (New England Biolabs, USA) was added, the mixture was incubated at 37 °C for 1 min, DNase was inactivated by incubation at 75° C for 15 min, and Rv0430 was denatured by heating at 95 °C for 20 min. The DNA products were analyzed by electrophoresis in 1% agarose gel with visualization using UV light after EtBr staining. Protection of DNA from degradation by peroxide was assessed by incubating pUC18 with 10 mM $FeSO_4$, 2.5 mM H_2O_2, and varying concentrations of Rv0430 in 1× EMSA buffer for 2 min at 25 °C. Reactions were stopped by the addition of 10 mM EDTA. Rv0430 was denatured by heating reaction mixtures to 95 °C for 20 min, and DNA products were analyzed by electrophoresis in 1% agarose gel with visualization using UV light after EtBr staining.

SELEX

SELEX was carried out with modifications described in Ref. [79]. A pool of random 18-mer double-stranded oligonucleotides, flanked on either side by M13 forward and reverse primer binding sites, was used as the starting SELEX library. For the first round of SELEX, 200 ng of the random SELEX library was incubated with hexa-histidine-tagged Rv0430 or MS_0833 in SELEX buffer [10 mM Tris–HCl (pH 7.4), 200 mM NaCl, 5% glycerol, 0.5 mM EDTA] at 25 °C for 1 h. Then Ni-NTA beads were added to the reactions and incubated for 40 min at 4 °C. As a bead-only control, Ni-NTA beads were incubated with the SELEX library. After collecting the beads by centrifugation (2000 rpm, 2 min), they were washed five times with 1 ml SELEX buffer and boiled with 100 μl water for 10 min for eluting DNA from the bead. Then 4 μl was taken as a template for a PCR-mediated amplification using M13 forward and reverse primers (Supplementary Table S1) and the following protocol per cycle for 20 cycles: 95 °C for 5 min, 95 °C for 30 s, 62.7 °C for 12 s, 72 °C for 7 s, and 72 °C for 5 min. For the next SELEX round, 10 μl of this PCR product was used for binding with Rv0430 and MS_0833. These steps were repeated until the sixth round. The enriched oligonucleotides from the sixth round of SELEX were inserted into the pGEMT-Easy vector (Promega, USA); correct insertion was confirmed by EcoRI digestion and sequences of the amplified oligonucleotides were obtained by nucleotide sequence analysis.

Filter binding assay

Oligonucleotides designated as SeL_1, SeL_2, and SeL_3 (Supplementary Table S1) were radiolabeled and annealed with SeL_1c, SeL_2c, and SeL_3c (Supplementary Table S1), as described above in the protocol for EMSA. The radiolabeled double-stranded oligonucleotides were incubated with varying concentrations of Rv0430 or MS_0833 in 1× EMSA buffer in a total reaction volume of 20 µl at 25 °C for 15 min. The reactions were spotted on 0.45-µm pore-size nitrocellulose filters (Millipore, USA) on a 12-well filtration apparatus. The filters were allowed to stand for 5 min, and they were then washed twice with 1× EMSA buffer (1 ml per wash). The filters were dried, and radioactivity was measured by scintillation counting.

DNA end-joining assay

pUC18, linearized by incubation with BamH1, was incubated with Rv0430 in 1× EMSA buffer at 25 °C for 20 min. Reaction mixtures were supplemented with ligase buffer (New England Biolabs, USA) and 0.25U of T4 DNA ligase (New England Biolabs, USA), followed by incubation at 25 °C for 30 min. The ligase was heat-inactivated by incubation of the reaction mixture for 10 min at 65 °C. The reaction products were analyzed by gel electrophoresis in1% agarose with visualization using UV light after EtBr staining.

AFM

Relaxed and linear pUC18 were incubated with Rv0430 or MS_0833 in AFM buffer [20 mM Tris–HCl (pH 7.4), 5 mM $MgCl_2$, and 50 mM NaCl] for 15 min at 25 °C. Aliquots (10 µl) were spotted on a freshly cleaved piece of V-1 Quality Mucosavite Mica (Electron Microscopy Science, USA) and kept at 25 °C for 30 min. Excess sample was removed by washing with 100 µl water; the mica piece was dried in a desiccator. Imaging was performed in the non-contact mode at a scan rate of 0.5 Hz with a silicon nitride cantilever of 40 N m^{-1} stiffness in a NX10, Park systems AFM instrument.

Topoisomerase I assay

Supercoiled pUC18 plasmid DNA was incubated with varying concentrations of Rv0430 for 20 min at 25 °C. Purified *Mtb* TopoI or *E. coli* TopoI were added to the DNA–protein mixture and incubated at 37 °C for 30 min. The reactions were stopped by heat inactivation of the topoisomerases at 68 °C for 10 min, mixtures were loaded on a 1.2% agarose gel (without EtBr) followed by electrophoresis for 7 h at 50 V. DNA was visualized using UV light after EtBr staining.

ChIP and quantitative PCR

ChIP was carried out as described in Ref. [80]. Briefly, *Mtb* H37Ra cultures ($OD_{600\ nm}$ 0.7) were fixed with 2% formaldehyde for 10 min and lysed using a Biorupter water bath sonicator (Diagenode, Belgium). This treatment sheared chromosomal DNA to 200–800 bp (checked on 0.8% agarose gel). Sheared DNA was immuno-precipitated with affinity-purified anti-Rv0430 antibody. After purification of the immuno-precipitated DNA, enrichment of Rv0430 at its promoter was determined by quantitative PCR using the primer pair Rv0430_107FP and Rv0430_107RP (Supplementary Table S1).

In vitro transcription

Promoter DNA upstream from the coding sequence of *rv0430* [81] was amplified by PCR using primers Rv0430_220usFP and Rv0430_50codRP (Supplementary Table S1). The product was ligated to pARN [82], linearized with SmaI to place the *rv0430* promoter upstream from a transcription terminator (*rv1324*) [83]. σA-enriched RNAP was purified from *M. smegmatis* overexpressing σA [82]. *In vitro* transcription assays were performed using supercoiled, relaxed, and linear templates (100 ng) by incubation with various concentrations of Rv0430, 200 nM RNAP, 100 µM NTPs, and 1 µCi α^{32}P UTP in transcription buffer [50 mM Tris–HCl (pH 8.0), 3 mM magnesium acetate, 100 µM EDTA, 100 µM DTT, 30 mM KCl, 50 µg ml^{-1} bovine serum albumen, 5% glycerol) on ice for 5 min, and then at 37 °C for 30 min. Reactions were terminated by the addition of stop buffer (95% formamide, 0.025% w/v bromophenol blue, 0.025% w/v xylene cyanol, 5 mM EDTA, 0.025% sodium dodecyl sulfate, 8 M urea) and inactivated at 95 °C for 5 min. The reactions were electrophoresed in a 6% urea-polyacrylamide gel, and analyzed with a phosphor imager (GE Healthcare, USA). The run-off transcripts were quantified using Image gauge ver. 2.3 software (Fujifilm).

Novobiocin treatment, RNA isolation, and quantitative RT-PCR

Mtb H37Ra cultures were grown to $OD_{600\ nm}$ = 0.6 and treated with novobiocin (Sigma-Aldrich, USA) at a concentration of 100 µg ml^{-1} for 24 h. Total RNA was extracted by the RNAzol method (Sigma-Aldrich, USA) as per the manufacturer's instructions. Total RNA of 10 ng was treated with RNase-free (Roche, Switzerland) to eliminate contaminating DNA. cDNA synthesis was carried out using Superscript III 25 °C (Invitrogen, USA). cDNA was diluted to the desired concentration, and quantitative PCR was carried out using 2× SYBR

mix (Fermentas, USA) as per the manufacturer's instructions in a thermal cycler (Applied Biosystems, USA).

CRediT authorship contribution statement

Chandreyee Datta: Conceptualization, Data curation, Investigation, Methodology, Writing - original draft, Writing - review & editing. **Rajiv Kumar Jha:** Data curation, Investigation, Methodology, Writing - review & editing. **Sohini Ganguly:** Data curation, Methodology, Writing - review & editing. **Valakunja Nagaraja:** Conceptualization, Data curation, Funding acquisition, Investigation, Project administration, Resources, Supervision, Writing - review & editing.

Acknowledgments

We are grateful to Prof. Karl Drlica and Soumitra Ghosh for critical input and helpful suggestions during preparation of the manuscript; we thank Monisha Mohandas of The Centre for Biosystems Science and Engineering, IISc for AFM experiments, and Rupesh Kumar and Adwait Anand Godbole for providing TopoNM and Topoiosomerase I enzymes, respectively. The central facility of phosphor imaging of Indian Institute of Science is acknowledged. This work is financially supported by DBT-IISc partnership program and grants from the Department of Biotechnology, Government of India (MCB/VNR/DBT/496, BT/PR27952/INF/22/212/2018) to V.N., who is a J.C. Bose Fellow of the Department of Science and Technology Government of India, as well as Life Science Research, Education and Training at JNCSAR, India (BT/INF/22/SP27679/2018).

Conflict of Interest Statement: The authors declare no conflict of interest with the contents of this article.

Appendix A. Supplementary data

Supplementary data to this article can be found online at https://doi.org/10.1016/j.jmb.2019.02.029.

Received 10 November 2018;
Received in revised form 23 February 2019;
Accepted 25 February 2019
Available online 12 March 2019

Keywords:
Mycobacterium tuberculosis;
nucleoid-associated protein (NAP);
DNA architecture;
transcription regulator

Abbreviations used:
NAP, nucleoid-associated protein; EMSA, electrophoretic mobility shift assay; AFM, atomic force microscopy; ChIP, chromatin immunoprecipitation; RST, relaxation stimulated transcription; PMSF, phenylmethylsulfonyl fluoride; EtBr, ethidium bromide; SELEX, selective evolution of ligand by exponential enrichment.

References

[1] S. Cunha, C.L. Woldringh, T. Odijk, Polymer-mediated compaction and internal dynamics of isolated *Escherichia coli* nucleoids, J. Struct. Biol. 136 (2001) 53–66.
[2] M. Joyeux, Compaction of bacterial genomic DNA: clarifying the concepts, J. Phys. Condens. Matter 27 (2015), 383001.
[3] R. de Vries, DNA compaction by nonbinding macromolecules, Polym. Sci. Ser. C 54 (2012) 30–35.
[4] R. de Vries, DNA condensation in bacteria: Interplay between macromolecular crowding and nucleoid proteins, Biochimie. 92 (2010) 1715–1721.
[5] R.T. Dame, The role of nucleoid-associated proteins in the organization and compaction of bacterial chromatin, Mol. Microbiol. 56 (2005) 858–870.
[6] S.C. Dillon, C.J. Dorman, Bacterial nucleoid-associated proteins, nucleoid structure and gene expression, Nat. Rev. Microbiol. 8 (2010) 185–195.
[7] S.P. Hancock, S. Stella, D. Cascio, R.C. Johnson, DNA sequence determinants controlling affinity, stability and shape of DNA complexes bound by the nucleoid protein Fis, PLoS One 11 (2016), e0150189.
[8] Y. Shao, L.S. Feldman-Cohen, R. Osuna, Functional characterization of the *Escherichia coli* Fis-DNA binding sequence, J. Mol. Biol. 376 (2008) 771–785.
[9] J.F. Gardner, H.A. Nash, Role of *Escherichia coli* IHF protein in lambda site-specific recombination: A mutational analysis of binding sites, J. Mol. Biol. 191 (1986) 181–189.
[10] K.K. Swinger, K.M. Lemberg, Y. Zhang, P.A. Rice, Flexible DNA bending in HU-DNA cocrystal structures, EMBO J. 22 (2003) 3749–3760.
[11] W.W. Navarre, S. Porwollik, Y. Wang, M. McClelland, H. Rosen, S.J. Libby, F.C. Fang, Selective silencing of foreign DNA with low GC content by the H-NS protein in *Salmonella*, Science. 313 (2006) 236–238.
[12] S. Lucchini, G. Rowley, M.D. Goldberg, D. Hurd, M. Harrison, J.C.D. Hinton, H-NS mediates the silencing of laterally acquired genes in bacteria, PLoS Pathog. 2 (2006) e81.
[13] V.S. Lioy, A. Cournac, M. Marbouty, S. Duigou, J. Mozziconacci, O. Espéli, F. Boccard, R. Koszul, Multiscale structuring of the *E. coli* chromosome by nucleoid-associated and condensin proteins, Cell. 172 (2018) (771-783.e18).
[14] M.S. Luijsterburg, M.C. Noom, G.J.L. Wuite, R.T. Dame, The architectural role of nucleoid-associated proteins in the organization of bacterial chromatin: a molecular perspective, J. Struct. Biol. 156 (2006) 262–272.
[15] P.M. Leonard, S.H. Smits, S.E. Sedelnikova, A.B. Brinkman, W.M. de Vos, J. van der Oost, D.W. Rice, J.B. Rafferty, Crystal structure of the Lrp-like transcriptional regulator from

the archaeon *Pyrococcus furiosus*, EMBO J. 20 (2001) 990–997.
[16] P.A. Rice, S. Yang, K. Mizuuchi, H.A. Nash, Crystal structure of an IHF–DNA complex: a protein-induced DNA U-turn, Cell. 87 (1996) 1295–1306.
[17] P. Thaw, S.E. Sedelnikova, T. Muranova, S. Wiese, S. Ayora, J.C. Alonso, A.B. Brinkman, J. Akerboom, J. van der Oost, J. B. Rafferty, Structural insight into gene transcriptional regulation and effector binding by the Lrp/AsnC family, Nucleic Acids Res. 34 (2006) 1439–1449.
[18] S. de los Rios, J.J. Perona, Structure of the *Escherichia coli* leucine-responsive regulatory protein Lrp reveals a novel octameric assembly, J. Mol. Biol. 366 (2007) 1589–1602.
[19] R.T. Dame, M.S. Luijsterburg, E. Krin, P.N. Bertin, R. Wagner, G.J.L. Wuite, DNA bridging: a property shared among H-NS-like proteins, J. Bacteriol. 187 (2005) 1845–1848.
[20] M.V. Kotlajich, D.R. Hron, B.A. Boudreau, Z. Sun, Y.L. Lyubchenko, R. Landick, Bridged filaments of histone-like nucleoid structuring protein pause RNA polymerase and aid termination in bacteria, Elife. 4 (2015), e04970.
[21] C. Prigent-Combaret, O. Zghidi-Abouzid, G. Effantin, P. Lejeune, S. Reverchon, W. Nasser, The nucleoid-associated protein Fis directly modulates the synthesis of cellulose, an essential component of pellicle-biofilms in the phytopathogenic bacterium *Dickeya dadantii*, Mol. Microbiol. 86 (2012) 172–186.
[22] R.L. Wilson, S.J. Libby, A.M. Freet, J.D. Boddicker, T.F. Fahlen, B.D. Jones, Fis, a DNA nucleoid-associated protein, is involved in *Salmonella typhimurium* SPI-1 invasion gene expression, Mol. Microbiol. 39 (2001) 79–88.
[23] T. Ó Cróinín, R.K. Carroll, A. Kelly, C.J. Dorman, Roles for DNA supercoiling and the Fis protein in modulating expression of virulence genes during intracellular growth of *Salmonella enterica* serovar Typhimurium, Mol. Microbiol. 62 (2006) 869–882.
[24] A. Hernday, M. Krabbe, B. Braaten, D. Low, Self-perpetuating epigenetic pili switches in bacteria, Proc. Natl. Acad. Sci. 99 (2002) 16470–16476.
[25] C. Lee, K.J. Marians, Characterization of the nucleoid-associated protein YejK, J. Biol. Chem. 288 (2013) 31503–31516.
[26] J. Teramoto, S.H. Yoshimura, K. Takeyasu, A. Ishihama, A novel nucleoid protein of *Escherichia coli* induced under anaerobiotic growth conditions, Nucleic Acids Res. 38 (2010) 3605–3618.
[27] T.A. Azam, A. Ishihama, Twelve species of the nucleoid-associated protein from *Escherichia coli*. Sequence recognition specificity and DNA binding affinity, J. Biol. Chem. 274 (1999) 33105–33113.
[28] D. Basu, G. Khare, S. Singh, A. Tyagi, S. Khosla, S.C. Mande, A novel nucleoid-associated protein of *Mycobacterium tuberculosis* is a sequence homolog of GroEL, Nucleic Acids Res. 37 (2009) 4944–4954.
[29] B. Blasco, J.M. Chen, R. Hartkoorn, C. Sala, S. Uplekar, J. Rougemont, F. Pojer, S.T. Cole, Virulence regulator EspR of *Mycobacterium tuberculosis* is a nucleoid-associated protein, PLoS Pathog. 8 (2012), e1002621.
[30] R. Colangeli, D. Helb, C. Vilchèze, M.H. Hazbón, C.-G. Lee, H. Safi, B. Sayers, I. Sardone, M.B. Jones, R.D. Fleischmann, S. N. Peterson, W.R. Jacobs, D. Alland, Transcriptional regulation of multi-drug tolerance and antibiotic-induced responses by the histone-like protein Lsr2 in *M. tuberculosis*, PLoS Pathog. 3 (2007) e87.
[31] S. Prabhakar, P.S. Annapurna, P.S. Annapurna, N.K. Jain, A. B. Dey, J.S. Tyagi, H.K. Prasad, Identification of an immunogenic histone-like protein (HLPMt) of *Mycobacterium tuberculosis*, Tuber. Lung Dis. 79 (1998) 43–53.
[32] S. Ghosh, S.S. Indi, V. Nagaraja, Regulation of lipid biosynthesis, sliding motility, and biofilm formation by a membrane-anchored nucleoid-associated protein of *Mycobacterium tuberculosis*, J. Bacteriol. 195 (2013) 1769–1778.
[33] Y. Liu, H. Wang, T. Cui, X. Zhou, Y. Jia, H. Zhang, Z.-G. He, NapM, a new nucleoid-associated protein, broadly regulates gene expression and affects mycobacterial resistance to anti-tuberculosis drugs, Mol. Microbiol. 101 (2016) 167–181.
[34] A. Mishra, M. Vij, D. Kumar, V. Taneja, A.K. Mondal, A. Bothra, V. Rao, M. Ganguli, B. Taneja, Integration host factor of *Mycobacterium tuberculosis*, mIHF, compacts DNA by a bending mechanism, PLoS One 8 (2013), e69985.
[35] D. Song, J.J. Loparo, Building bridges within the bacterial chromosome, Trends Genet. 31 (2015) 164–173.
[36] D.I. Friedman, Integration host factor: a protein for all reasons, Cell. 55 (1988) 545–554.
[37] S.S. Ali, B. Xia, J. Liu, W.W. Navarre, Silencing of foreign DNA in bacteria, Curr. Opin. Microbiol. 15 (2012) 175–181.
[38] L.N. Calhoun, Y.M. Kwon, Structure, function and regulation of the DNA-binding protein Dps and its role in acid and oxidative stress resistance in *Escherichia coli*: a review, J. Appl. Microbiol. 110 (2011) 375–386.
[39] A. Grove, Functional evolution of bacterial histone-like HU proteins, Curr. Issues Mol. Biol. 13 (2011) 1–12.
[40] A. Free, R.M. Williams, C.J. Dorman, The StpA protein functions as a molecular adapter to mediate repression of the *bgl* operon by truncated H-NS in *Escherichia coli*, J. Bacteriol. 180 (1998) 994–997.
[41] C.M. Müller, U. Dobrindt, G. Nagy, L. Emödy, B.E. Uhlin, J. Hacker, Role of histone-like proteins H-NS and StpA in expression of virulence determinants of uropathogenic *Escherichia coli*, J. Bacteriol. 188 (2006) 5428–5438.
[42] G.M. Cech, A. Szalewska-Pałasz, K. Kubiak, A. Malabirade, W. Grange, V. Arluison, G. Węgrzyn, The *Escherichia Coli* Hfq protein: an unattended DNA-transactions regulator, Front. Mol. Biosci. 3 (2016) 36.
[43] T. Bhowmick, S. Ghosh, K. Dixit, V. Ganesan, U.A. Ramagopal, D. Dey, S.P. Sarma, S. Ramakumar, V. Nagaraja, Targeting *Mycobacterium tuberculosis* nucleoid-associated protein HU with structure-based inhibitors, Nat. Commun. 5 (2014) 4124.
[44] F. Boubrik, J. Rouviere-Yaniv, Increased sensitivity to gamma irradiation in bacteria lacking protein HU, Proc. Natl. Acad. Sci. U. S. A. 92 (1995) 3958–3962.
[45] J.E. Griffin, J.D. Gawronski, M.A. DeJesus, T.R. Ioerger, B.J. Akerley, C.M. Sassetti, High-resolution phenotypic profiling defines genes essential for mycobacterial growth and cholesterol catabolism, PLoS Pathog. 7 (2011), e1002251.
[46] C.M. Sassetti, D.H. Boyd, E.J. Rubin, Genes required for mycobacterial growth defined by high density mutagenesis, Mol. Microbiol. 48 (2003) 77–84.
[47] S. Karambelkar, G. Swapna, V. Nagaraja, Silencing of toxic gene expression by Fis, Nucleic Acids Res. 40 (2012) 4358–4367.
[48] R. Colangeli, A. Haq, V.L. Arcus, E. Summers, R.S. Magliozzo, A. McBride, A.K. Mitra, M. Radjainia, A. Khajo, W.R. Jacobs, P. Salgame, D. Alland, The multifunctional histone-like protein Lsr2 protects mycobacteria against reactive oxygen intermediates, Proc. Natl. Acad. Sci. 106 (2009) 4414–4418.
[49] A. Martinez, R. Kolter, Protection of DNA during oxidative stress by the nonspecific DNA-binding protein Dps, J. Bacteriol. 179 (1997) 5188–5194.

[50] S. Ghosh, B. Mallick, V. Nagaraja, Direct regulation of topoisomerase activity by a nucleoid-associated protein, Nucleic Acids Res. 42 (2014) 11156–11165.
[51] K. Drlica, M. Snyder, Superhelical *Escherichia coli* DNA: relaxation by coumermycin, J. Mol. Biol. 120 (1978) 145–154.
[52] R. Menzel, M. Gellert, Regulation of the genes for *E. coli* DNA gyrase: homeostatic control of DNA supercoiling, Cell. 34 (1983) 105–113.
[53] S. Unniraman, M. Chatterji, V. Nagaraja, DNA gyrase genes in *Mycobacterium tuberculosis*: a single operon driven by multiple promoters, J. Bacteriol. 184 (2002) 5449–5456.
[54] T.B.K. Le, M.V. Imakaev, L.A. Mirny, M.T. Laub, High-resolution mapping of the spatial organization of a bacterial chromosome, Science. 342 (2013) 731–734.
[55] X. Wang, P.M. Llopis, D.Z. Rudner, Organization and segregation of bacterial chromosomes, Nat. Rev. Genet. 14 (2013) 191–203.
[56] B.-K. Cho, E.M. Knight, C.L. Barrett, B.O. Palsson, Genome-wide analysis of Fis binding in *Escherichia coli* indicates a causative role for A-/AT-tracts, Genome Res. 18 (2008) 900–910.
[57] K. Chintakayala, S.S. Singh, A.E. Rossiter, R. Shahapure, R.T. Dame, D.C. Grainger, *E. coli* Fis protein insulates the *cbpA* gene from uncontrolled transcription, PLoS Genet. 9 (2013), e1003152.
[58] B.R.G. Gordon, Y. Li, L. Wang, A. Sintsova, H. van Bakel, S. Tian, W.W. Navarre, B. Xia, J. Liu, Lsr2 is a nucleoid-associated protein that targets AT-rich sequences and virulence genes in *Mycobacterium tuberculosis*, Proc. Natl. Acad. Sci. U. S. A. 107 (2010) 5154–5159.
[59] J. Becq, M.C. Gutierrez, V. Rosas-Magallanes, J. Rauzier, B. Gicquel, O. Neyrolles, P. Deschavanne, Contribution of horizontally acquired genomic islands to the evolution of the tubercle bacilli, Mol. Biol. Evol. 24 (2007) 1861–1871.
[60] J. Koh, R.M. Saecker, M.T. Record, DNA binding mode transitions of *Escherichia coli* HUαβ: evidence for formation of a bent DNA–protein complex on intact, linear duplex DNA, J. Mol. Biol. 383 (2008) 324–346.
[61] N. Laurens, R.P.C. Driessen, I. Heller, D. Vorselen, M.C. Noom, F.J.H. Hol, M.F. White, R.T. Dame, G.J.L. Wuite, Alba shapes the archaeal genome using a delicate balance of bridging and stiffening the DNA, Nat. Commun. 3 (2012) 1328.
[62] F. Guo, S. Adhya, Spiral structure of *Escherichia coli* HUalphabeta provides foundation for DNA supercoiling, Proc. Natl. Acad. Sci. U. S. A. 104 (2007) 4309–4314.
[63] S. Kar, E.J. Choi, F. Guo, E.K. Dimitriadis, S.L. Kotova, S. Adhya, Right-handed DNA supercoiling by an octameric form of histone-like protein HU: modulation of cellular transcription, J. Biol. Chem. 281 (2006) 40144–40153.
[64] S. Kar, R. Edgar, S. Adhya, Nucleoid remodeling by an altered HU protein: reorganization of the transcription program, Proc. Natl. Acad. Sci. 102 (2005) 16397–16402.
[65] A. Travers, G. Muskhelishvili, DNA microloops and microdomains: a general mechanism for transcription activation by torsional transmission, J. Mol. Biol. 279 (1998) 1027–1043.
[66] G. Muskhelishvili, M. Buckle, H. Heumann, R. Kahmann, A.A. Travers, FIS activates sequential steps during transcription initiation at a stable RNA promoter, EMBO J. 16 (1997) 3655–3665.
[67] C.J. Dorman, DNA supercoiling and bacterial gene expression, Sci. Prog. 89 (2006) 151–166.
[68] C.J. Dorman, N. Ní Bhriain, DNA topology and bacterial virulence gene regulation, Trends Microbiol. 1 (1993) 92–99.
[69] C.J. Dorman, Co-operative roles for DNA supercoiling and nucleoid-associated proteins in the regulation of bacterial transcription, Biochem. Soc. Trans. 41 (2013) 542–547.
[70] Z.-A. Ouafa, S. Reverchon, T. Lautier, G. Muskhelishvili, W. Nasser, The nucleoid-associated proteins H-NS and FIS modulate the DNA supercoiling response of the *pel* genes, the major virulence factors in the plant pathogen bacterium *Dickeya dadantii*, Nucleic Acids Res. 40 (2012) 4306–4319.
[71] A. Duprey, S. Reverchon, W. Nasser, Bacterial virulence and Fis: adapting regulatory networks to the host environment, Trends Microbiol. 22 (2014) 92–99.
[72] I.L. Bartek, L.K. Woolhiser, A.D. Baughn, R.J. Basaraba, W. R. Jacobs, A.J. Lenaerts, M.I. Voskuil, *Mycobacterium tuberculosis* Lsr2 is a global transcriptional regulator required for adaptation to changing oxygen levels and virulence, MBio. 5 (2014) e01106–e01114.
[73] D.M. Hunt, N.P. Sweeney, L. Mori, R.H. Whalan, I. Comas, L. Norman, T. Cortes, K.B. Arnvig, E.O. Davis, M.R. Stapleton, J. Green, R.S. Buxton, Long-range transcriptional control of an operon necessary for virulence-critical ESX-1 secretion in *Mycobacterium tuberculosis*, J. Bacteriol. 194 (2012) 2307–2320.
[74] P. Rath, C. Huang, T. Wang, T. Wang, H. Li, R. Prados-Rosales, O. Elemento, A. Casadevall, C.F. Nathan, Genetic regulation of vesiculogenesis and immunomodulation in *Mycobacterium tuberculosis*, Proc. Natl. Acad. Sci. 110 (2013) E4790–E4797.
[75] A.M. Beaulieu, P. Rath, M. Imhof, M.E. Siddall, J. Roberts, D. Schnappinger, C.F. Nathan, Genome-wide screen for *Mycobacterium tuberculosis* genes that regulate host Immunity, PLoS One 5 (2010), e15120.
[76] M. D'orazio, S. Folcarelli, F. Mariani, V. Colizzi, G. Rotilio, A. Battistoni, Lipid modification of the Cu,Zn superoxide dismutase from *Mycobacterium tuberculosis*, Biochem. J. 359 (2001) 17–22.
[77] D.L. Piddington, F.C. Fang, T. Laessig, A.M. Cooper, I.M. Orme, N.A. Buchmeier, Cu,Zn superoxide dismutase of *Mycobacterium tuberculosis* contributes to survival in activated macrophages that are generating an oxidative burst, Infect. Immun. 69 (2001) 4980–4987.
[78] E. Volpe, G. Cappelli, M. Grassi, A. Martino, A. Serafino, V. Colizzi, N. Sanarico, F. Mariani, Gene expression profiling of human macrophages at late time of infection with *Mycobacterium tuberculosis*, Immunology. 118 (2006) 449–460.
[79] D. Feltkamp, F.F. Wiebel, S. Alberti, J.A. Gustafsson, Identification of a novel DNA binding site for nuclear orphan receptor OR1, J. Biol. Chem. 274 (1999) 10421–10429.
[80] S. Uplekar, J. Rougemont, S.T. Cole, C. Sala, High-resolution transcriptome and genome-wide dynamics of RNA polymerase and NusA in *Mycobacterium tuberculosis*, Nucleic Acids Res. 41 (2013) 961–977.
[81] T. Cortes, O.T. Schubert, G. Rose, K.B. Arnvig, I. Comas, R. Aebersold, D.B. Young, Genome-wide mapping of transcriptional start sites defines an extensive leaderless transcriptome in *Mycobacterium tuberculosis*, Cell Rep. 5 (2013) 1121–1131.
[82] A. China, S. Mishra, P. Tare, V. Nagaraja, Inhibition of *Mycobacterium tuberculosis* RNA polymerase by binding of a Gre factor homolog to the secondary channel, J. Bacteriol. 194 (2012) 1009–1017.
[83] S. Unniraman, R. Prakash, V. Nagaraja, Alternate paradigm for intrinsic transcription termination in eubacteria, J. Biol. Chem. 276 (2001) 41850–41855.